A Probabilistic Framework for Reserve Scheduling and N − 1 Security Assessment of Systems With High Wind Power Penetration

Maria Vrakopoulou, *Student Member, IEEE*, Kostas Margellos, *Student Member, IEEE*, John Lygeros, *Fellow, IEEE*, and Göran Andersson, *Fellow, IEEE*

***Abstract*—We propose a probabilistic framework to design an N − 1 secure day-ahead dispatch and determine the minimum cost reserves for power systems with wind power generation. We also identify a reserve strategy according to which we deploy the reserves in real-time operation, which serves as a corrective control action. To achieve this, we formulate a stochastic optimization program with chance constraints, which encode the probability of satisfying the transmission capacity constraints of the lines and the generation limits. To incorporate a reserve decision scheme, we take into account the steady-state behavior of the secondary frequency controller and, hence, consider the deployed reserves to be a linear function of the total generation-load mismatch. The overall problem results in a chance constrained bilinear program. To achieve tractability, we propose a convex reformulation and a heuristic algorithm, whereas to deal with the chance constraint we use a scenario-based-approach and an approach that considers only the quantiles of the stationary distribution of the wind power error. To quantify the effectiveness of the proposed methodologies and compare them in terms of cost and performance, we use the IEEE 30-bus network and carry out Monte Carlo simulations, corresponding to different wind power realizations generated by a Markov chain-based model.**

***Index Terms*—Chance-constrained optimization, corrective security, N − 1 security, reserve scheduling, wind power integration.**

I. Introduction

THE expected increase in the installed wind power capacity and other fluctuating power sources as well (e.g., photovoltaic power) highlights the necessity of revisiting certain operational concepts, like security and reserve scheduling. In a deterministic setup, security of a power system refers to its ability to withstand contingencies without disruption of service [1], [2]. As a security measure, the N − 1 security criterion is commonly used, under which the system is considered to be secure if any single component outage does not lead to any operational violations.

In the absence of uncertainty, many methods dealing with security enhancement have been proposed [3]–[7]. From a market point of view, the authors of [8] propose a method for incorporating contingencies and stability constraints by making use of a voltage-constrained optimal power flow. On the other hand, in the presence of uncertainty, most of the research has either concentrated on the economic implications of security [9], [10] or has resorted to Monte Carlo-based statistical analyses [11], [12]. Toward maximizing the expected social welfare, optimization of reserve power has been addressed in [13]–[16] in a security-constrained market clearing context. Using the same framework, the work in [17] and [18] formulated a multistage stochastic unit commitment program, modeling the uncertain generation by means of scenarios and using reduction techniques to ensure tractability of the problem. However, these approaches do not offer *a priori* guarantees regarding the reliability of the resulting solution.

In this paper, we propose a unified framework that simultaneously solves the problem of designing an N − 1 secure day-ahead dispatch for the generating units while determining the minimum cost reserves and the optimal way to deploy them. To account for the variability of wind power, we follow a probabilistic methodology, providing certain guarantees regarding the satisfaction of the system constraints. We first integrate, as in [19], the security constraints emanating from the N − 1 criterion to a dc optimal power flow problem and formulate a stochastic optimization problem with chance constraints. Modeling the steady-state behavior of the secondary frequency controller leads to a representation of the reserves as a linear function of the total generation-load mismatch, which may be due either to the difference between the actual wind and its forecast or to a generator/load loss. We introduce different ways to distribute reserves based on the type of mismatch, thus offering an implementation of corrective security. Therefore, the overall formulation includes both preventive and corrective control [20]. The generation dispatch and the reserve capacity determination consist of preventive control actions, whereas the case-dependent strategy according to which we deploy reserves in real-time operation falls in the framework of corrective control. Apart from the physical intuition, using such a strategy for the reserves has the advantage that the number of decision variables does not grow with the number of uncertainty realizations as in [17], and

Manuscript received August 06, 2012; revised December 20, 2012; accepted June 17, 2013. Date of publication July 29, 2013; date of current version October 17, 2013. This work was supported in part by the European Commission under Project MoVeS, FP7-ICT-257005, the Network of Excellence HYCON2, FP7-ICT-257462, the KIOS Center of Excellence 0308/28 and the Swiss Secretariat for Education and Research under a project within COST-Action IC0806. Paper no. TPWRS-00919-2012.

M. Vrakopoulou and G. Andersson are with the Power Systems Laboratory, Department of Electrical Engineering, ETH Zürich, 8092 Zürich, Switzerland (e-mail: vrakopoulou@eeh.ee.ethz.ch; andersson@eeh.ee.ethz.ch).

K. Margellos, and J. Lygeros are with the Automatic Control Laboratory, Department of Electrical Engineering, ETH Zürich, 8092 Zürich, Switzerland (e-mail: margellos@control.ee.ethz.ch; lygeros@control.ee.ethz.ch).

Color versions of one or more of the figures in this paper are available online at http://ieeexplore.ieee.org.

Digital Object Identifier 10.1109/TPWRS.2013.2272546

the resulting solution is less conservative compared with that of [21]. This makes our method applicable even for large-scale networks.

The resulting problem is a chance-constrained bilinear program. To achieve tractability, the issues arising due to the bilinear terms and the presence of the chance constraint need to be resolved. To alleviate these difficulties, we propose a heuristic algorithm and a convex reformulation, as well as two alternative techniques to deal with the chance constraint. The effectiveness of the proposed methodologies is illustrated by means of Monte Carlo simulations for a modified version of the IEEE 30-bus network [22].

In Section II, we formulate the security constrained reserve scheduling problem as a chance constrained optimization program. Section III provides details on how to deal with the bilinearity problem and the chance constraint, and Section IV illustrates the performance of the proposed approaches via a simulation study. Finally, in Section V, we provide some directions for future work.

II. Problem Formulation

A. Problem Setup and Definitions

We consider a power network comprising N_G generating units, N_L loads, N_l lines, and N_b buses. For the security-constrained formulation, as in [13] and [23], we take into account any outage involving the tripping of a branch, generator, or load, and by $N_{out} = N_l + N_G + N_L$ we denote the total number of possible single outages. Moreover, denote by $\mathcal{I}_l, \mathcal{I}_L, \mathcal{I}_G$ the set of indices corresponding to branch, load, and generator outages. The "0" index corresponds to the case of no outage. Let also $\mathcal{I} = \{0\} \cup \mathcal{I}_l \cup \mathcal{I}_L \cup \mathcal{I}_G$.

The problem formulation of the next section is based on the following assumptions: 1) a standard dc power flow approximation [24] is used; 2) wind generation is located at a single bus of the network; 3) perfect load forecasts are considered; 4) line outages do not lead to multiple generator/load failures; and 5) the "ON–OFF" status of the generating units has been fixed *a priori* by solving a unit-commitment problem. The first assumption is standard for this type of problems. The second, third, and fourth are included to simplify the presentation of our results and could still be captured by the proposed algorithm. Removing the last assumption by incorporating the unit commitment problem would give rise to a mixed-integer problem; this can be tackled using the modified version of the scenario approach [25], as will be discussed in Section III-C1.

Under the dc power flow approximation and by eliminating the angles by setting the reference angle to zero [19], the vector including the power flows across each line can be defined as $P^i_{fl} = B^i_{fl}\left[(\widetilde{B}^i_{BUS})^{-1}\widetilde{P}^i \quad 0\right]^T \in \mathbb{R}^{N_l}$, where the power injection vector $\widetilde{P}^i$ is given by

$$\widetilde{P}^i = \left[I^i_G C_G(P_G + R^i) + C_w P_w - I^i_L C_L P_L\right]_{N_b-1} \in \mathbb{R}^{N_b-1} \tag{1}$$

where $[\cdot]_{N_b-1}$ denotes the first N_b-1 rows of the quantity inside the brackets. For every outage, matrices B^i_{fl} and B^i_{BUS} denote the imaginary part of the admittance of each network branch and the nodal admittance matrix. $P_G \in \mathbb{R}^{N_G}$, $P_w \in \mathbb{R}$, and $P_L \in \mathbb{R}^{N_L}$ denote the generation dispatch, the wind power in-feed, and the load, respectively. $R^i \in \mathbb{R}^{N_G}$ is a power correction term, which is related to the reserves provided by each generator and will be defined in Section II-B. Matrices C_G, C_w, and C_L are of appropriate dimension, and their element (i, j) is "1" if generator j (resp. wind power/load) is connected to the bus i and zero otherwise. Matrices $I^i_G \in \mathbb{R}^{N_b \times N_b}$, $I^i_L \in \mathbb{R}^{N_b \times N_b}$ depend on the outage i. Specifically, for $i \in \{0\} \cup \mathcal{I}_l \cup \mathcal{I}_L$ (i.e., the case where we have no generator outage), $I^i_G \in \mathbb{R}^{N_b \times N_b}$ (similarly for $I^i_L \in \mathbb{R}^{N_b \times N_b}$) is an identity matrix, where for $i \in \mathcal{I}_G$ the diagonal element with index corresponding to the bus to which the tripped generator is connected is set to zero.

B. Reserves Representation

Reserves are needed to balance generation-load mismatches, which may occur due to a difference between the actual wind power and its forecast or as an effect of a generator/load loss. Such mismatches between load and generation induce frequency deviations and activate the primary and secondary frequency controllers [by means of automatic generation control (AGC)]. Here, we assume an ideal primary frequency control functionality compensating for any fast time-scale power deviation and focus only on the steady-state behavior of the AGC actions (and, hence, on the secondary frequency control reserves). The AGC output is distributed to certain participating generators, whose setpoint is changed by a certain percentage of the active power to be compensated. The product of these percentage weights with the worst case imbalance results in the amount of reserves that each generating unit has to provide. We will refer to the vector that includes these weights as the *distribution vector*.

The existing setup of the AGC loop is shown in Fig. 1, demonstrating the role of the distribution vector. In current practice, this vector results from the market that determines the secondary frequency control reserves and remains constant until the next market auction. Typically, this task is performed without taking the network constraints into account. Moreover, the distribution vector may differ between up-spinning and down-spinning reserves, but is the same for all possible outages. In this paper, in view of a corrective security control scheme, apart from distinguishing between up-spinning and down-spinning reserves, we also consider different distribution vectors depending on the outage. Optimizing then over the distribution vectors, we determine an optimal reserve schedule while taking the network security constraints into account. Our approach enables us to compute simultaneously both the minimum cost reserves per generator and a reserve strategy that can be deployed in real-time operation. This strategy consists of using the distribution vectors, which depending on the outage and the wind power deviation dictate the amount of power by which each generating unit should adjust its production. Therefore, the proposed methodology serves as an alternative to other methods for reserve scheduling, e.g., [17] and [18], which account implicitly for real-time response via their day-ahead decisions.

To encode the proposed reserve representation, we define a power correction term R^i as a linear function of the total generation-load mismatch. This term is directly related to the reserves

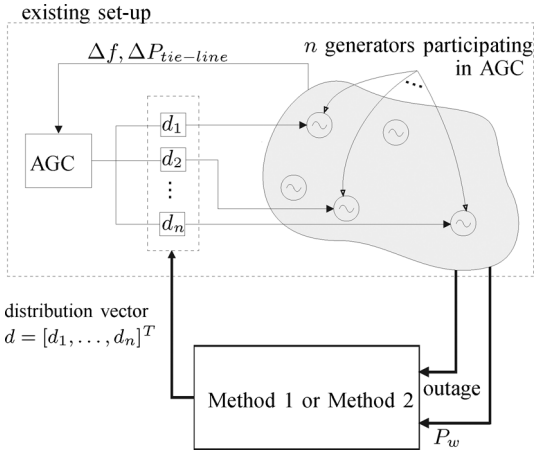

Fig. 1. Schematic diagram illustrating the AGC functionality required for the security-constrained reserve scheduling algorithm.

since it shows the amount of the reserves that, for every mismatch, will be provided by each generator:

$$R^i = d^i_{\text{up}} \max_{+}(-P^i_m) - d^i_{\text{down}} \max_{+}(P^i_m), \qquad \text{for all } i \in \mathcal{I} \tag{2}$$

where $\max_+(\cdot) = \max(\cdot, 0)$. Variable $P^i_m \in \mathbb{R}$ denotes the generation-load mismatch, which for each outage is given by

$$P^i_m = \begin{cases} P_w - P^f_w, & \text{if } i \in \mathcal{I}_l \text{ or } i = 0 \\ P_w - P^f_w + P^i_L, & \text{if } i \in \mathcal{I}_L \\ P_w - P^f_w - P^i_G, & \text{if } i \in \mathcal{I}_G \ . \end{cases} \tag{3}$$

Note that $P^i_L, P^i_G \in \mathbb{R}$ denote the element of $P_L \in \mathbb{R}^{N_L}$, $P_G \in \mathbb{R}^{N_G}$, that corresponds to the failed component i. Vectors $d^i_{\text{up}}, d^i_{\text{down}} \in \mathbb{R}^{N_G}$ represent the distribution vectors. The sum of their elements is equal to one and, if a generator is not contributing to the AGC, the corresponding element in the vector is zero. The indices up and down are used to distinguish between up-spinning and down-spinning reserves.

If P^i_m is negative, up-spinning reserves are provided and the production of the generators is increased accordingly, whereas in the opposite case the second term of (2) is active and, hence, down-spinning reserves are provided. Notice that d^i_{up}, d^i_{down}, $i \in \mathcal{I}$ may have negative elements as well. Consider for example the base case where we have no outages: the power mismatch is negative ($P^0_m < 0$), and some elements of d^0_{up} are negative as well. This corresponds to a setup where the network is congested. The interpretation of some elements of d^0_{up} being negative is that the corresponding generators should provide down-spinning reserves so that congestion is relieved, while the rest of the units would provide up-spinning reserves.

C. Probabilistic Security Constrained Reserve Scheduling

We consider an optimization horizon $T = 24$ with hourly steps,[1] and introduce the subscript t to indicate the value of the quantities for a given time instance $t = 1, \ldots, T$. We consider a quadratic form for the production cost and a linear cost for the reserves. Let $C_1, C_2, C_{\text{up}}, C_{\text{down}} \in \mathbb{R}^{N_G}$ be generation and reserve cost vectors and let $[C_2]$ denote a diagonal matrix with vector C_2 on the diagonal.

For each step t, define the vector of decision variables to be

$$x_t = [P_{G,t},\ [d^i_{\text{up},t}, d^i_{\text{down},t}, R^i_{\text{up},t}, R^i_{\text{down},t}]_{i\in\mathcal{I}}]^T \in \mathbb{R}^{N_G + 4N_G(N_{\text{out}}+1)},$$

where $R^i_{\text{up},t}, R^i_{\text{down},t} \in \mathbb{R}^{N_G}$ denote the probabilistically worst case up-down spinning reserves that the system operator needs to purchase for every $i \in \mathcal{I}$. The resulting optimization problem is

$$\min_{\{x_t\}_{t=1}^T} \sum_{t=1}^{T} \Big(C_1^T P_{G,t} + P_{G,t}^T [C_2] P_{G,t} + \sum_{i=0}^{N_{\text{out}}} \left(C^T_{\text{up}} R^i_{\text{up},t} + C^T_{\text{down}} R^i_{\text{down},t} \right) \Big) \tag{4}$$

subject to the following.

1) Forecast power balance constraints: for all $t = 1, \ldots, T$,

$$\mathbf{1}^T (C_G P_{G,t} + C_w P^f_{w,t} - C_L P_{L,t}) = 0. \tag{5}$$

This constraint encodes the fact that the power balance in the network should always be satisfied when $P_{w,t} = P^f_{w,t}$.

2) Generation limits: for all $t = 1, \ldots, T$

$$P_{\min} \le P_{G,t} \le P_{\max}, \tag{6}$$

where $P_{\min}, P_{\max} \in \mathbb{R}^{N_G}$ denote the minimum and maximum generating capacity of each unit.

3) Distribution vector constraints: for all $t = 1, \ldots, T$ and for all $i \in \mathcal{I}$

$$\mathbf{1}^T d^i_{\text{up},t} = 1, \mathbf{1}^T d^i_{\text{down},t} = 1. \tag{7}$$

For $i \in \mathcal{I}_G$, the element of $d^i_{\text{up},t}$, $d^i_{\text{down},t}$ corresponding to the tripped generator is equal to zero. Constraints (7) encode the fact that the elements of the distribution vectors should sum to one.

4) Probabilistic constraints: for all $t = 1, \ldots, T$

$$\mathbb{P}\Big(P_{w,t} \in \mathbb{R} | \ -\overline{P}^i_{\text{line}} \le B^i_{fl} \begin{bmatrix} (\widetilde{B}^i_{\text{BUS}})^{-1} \widetilde{P}^i_t \\ 0 \end{bmatrix} \overline{P}^i_{\text{line}}, \ P_{\min} \le P^i_{G,t} + R^i_t \le P_{\max}, \ -R^i_{\text{down},t} \le R^i_t \le R^i_{\text{up},t}, \ R^i_{\text{up},t}, R^i_{\text{down},t} \ge 0, \text{for } i \in \mathcal{I} \Big) \ge 1 - \epsilon \tag{8}$$

where the probability is meant with respect to the probability distribution of the wind power vector $P_{w,t} \in \mathbb{R}$. The first constraint inside the probability denotes the standard transmission capacity constraints for each outage i. $\overline{P}^i_{\text{line}}$ represents either normal or emergency line ratings. The second constraint provides guarantees that the scheduled generation dispatch plus the power correction term R^i_t will not result in a new operating point outside the generation capacity limits. The last constraint in (8) is included

[1]Here, we implicitly assume an ideal primary frequency control performance, capturing the fast time scale wind power variability. This is standard practice for day-ahead planning problems of this type [16]–[18].

to determine the reserves $R^i_{\text{up},t}$, $R^i_{\text{down},t}$ as the worst case, in a probabilistic sense, value of the power correction term R^i_t. The reserves that the system operator will need to purchase are then determined as $R_{\text{up},t} = \max_{i\in\mathcal{I}} R^i_{\text{up},t}$ and $R_{\text{down},t} = \max_{i\in\mathcal{I}} R^i_{\text{down},t}$, which denote the worst case values of $R^i_{\text{up},t}$ and $R^i_{\text{down},t}$, respectively. Note that in (8) we considered the same probability level ϵ for each time-step $t = 1,\ldots,T$, but different probability levels per stage or a joint chance constraint for all stages could be captured by the proposed framework as well.

Following this formulation, we propose an additional AGC functionality. The operator of the system needs to monitor both the production of the tripped plant and the deviation of the wind power from its forecast and, using (2) as a lookup table (LUT), select the appropriate distribution vector, among those computed in the optimization problem (see Fig. 1).

The resulting problem (1)–(8) is a chance-constrained bilinear program whose stages are only coupled due to the temporal correlation of the wind power. We could have a further coupling among the stages if a unit commitment problem was included or if ramping constraints of the generating units and minimum up and down times were modeled. The reader is referred to [26] for a setup where all of these constraints are included. There are two main challenges when attempting to solve problem (1)–(8). The first arises from the presence of bilinear terms due to the products of $d^i_{\text{up},t}$, $d^i_{\text{down},t}$ and $P_{G,t}$ for $i \in \mathcal{I}_G$, whereas the second is due to the presence of the chance constraint. These issues are addressed in Section III.

Algorithm 1

1: **Initialization – Part 1**.
2: Set $P^0_{G,t}$ (e.g., $P^0_{G,t} = 0$),3: $k = 1$.
4: **Repeat until convergence**

5: Set $P^{k,i}_{G,t} = P^{k-1,i}_{G,t}$, $\forall i \in \mathcal{I}_G$, *only* in **(2)**,
6: Compute x^k_t solving **(1)–(8)**,
7: Update $P^k_{G,t}$,
8: $k = k + 1$.

9: **end**
10: **Return converged solution** $x^{k^*}_t$
11: **Initialization – Part 2**.
12: Set $d^{0,i}_{\text{up},t} = d^{k^*,i}_{\text{up},t}$, $d^{0,i}_{\text{down},t} = d^{k^*,i}_{\text{down},t}$, $\forall i \in \mathcal{I}_G$,
13: $k = 1$.
14: **Repeat until convergence**

15: Set $d^{k,i}_{\text{up},t} = d^{k-1,i}_{\text{up},t}$, $d^{k,i}_{\text{down},t} = d^{k-1,i}_{\text{down},t}$, $\forall i \in \mathcal{I}_G$, in **(2)**,
16: Compute $\left[P^k_{G,t}, [d^{k,i}_{\text{up},t}, d^{k,i}_{\text{down},t}]_{i\in\mathcal{I}\setminus\mathcal{I}_G}, [R^{k,i}_{\text{up},t}, R^{k,i}_{\text{down},t}]_{i\in\mathcal{I}}\right]^T$ solving **(1)–(8)**,
17: Fix $P^k_{G,t}$ in **(1)–(8)**,
18: Compute $\left[[d^{k,i}_{\text{up},t}, d^{k,i}_{\text{down},t}, R^{k,i}_{\text{up},t}, R^{k,i}_{\text{down},t}]_{i\in\mathcal{I}}\right]^T$ solving **(1)–(8)**,
19: $k = k + 1$.

20: **end**

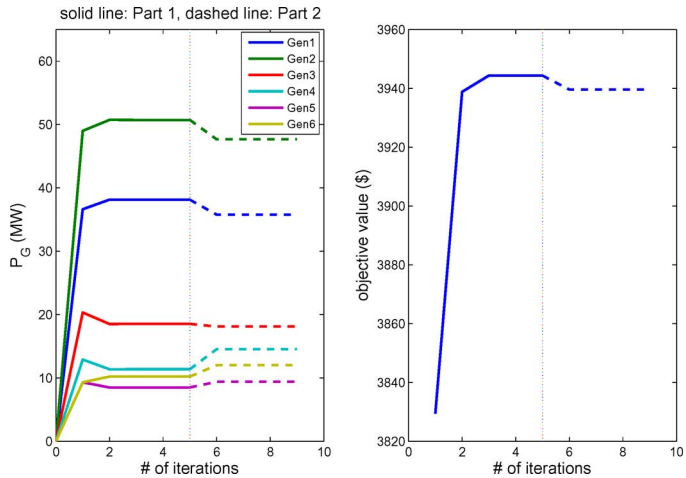

Fig. 2. Illustration of Algorithm 1 for 1 h of the simulated data, initialized with $P^0_{G,t} = 0$. For the first part, the power dispatch of each unit and the obtained objective value converge after three iterations, whereas for the second only one iteration is needed.

III. Tractable Problem Reformulations

A. Method 1: Heuristic Algorithm

We propose here a method based on an iterative algorithm (Algorithm 1) to deal with the bilinear terms. We first attempt to identify a feasible solution to the problem starting from an arbitrarily chosen power schedule $P^0_{G,t}$. For the simulation study of Section IV, we used $P^0_{G,t} = 0$; we have tested other initial values as well, and in all cases the algorithm converged to the same solution. At iteration k of the algorithm, we fix $P^{k,i}_{G,t}$ *only* in (2) to the value obtained in the previous iteration. Therefore, R^i is still a function of the distribution vectors and the production, but this time the value of the power production term is fixed to P^0_G to avoid the presence of bilinear terms. Solving then (1)–(8), a new solution x^k_t is computed and $P^k_{G,t}$ is updated accordingly. If the algorithm converges, its fixed point $x^{k^*}_t$ will be a feasible solution.

At a second step, we use an alternating scheme to refine the resulting feasible solution in terms of cost. At iteration k we first fix $d^{k,i}_{\text{up},t}$, $d^{k,i}_{\text{down},t}$ to the values obtained at the previous step of the algorithm *only* for $i \in \mathcal{I}_G$ and obtain $\left[P^k_{G,t}, [d^{k,i}_{\text{up},t}, d^{k,i}_{\text{down},t}]_{i\in\mathcal{I}\setminus\mathcal{I}_G}, [R^{k,i}_{\text{up},t}, R^{k,i}_{\text{down},t}]_{i\in\mathcal{I}}\right]^T$ by solving (1)–(8). We then fix $P^k_{G,t}$ to the computed value in all equations it appears and solve for the decision vector $\left[[d^{k,i}_{\text{up},t}, d^{k,i}_{\text{down},t}, R^{k,i}_{\text{up},t}, R^{k,i}_{\text{down},t}]_{i\in\mathcal{I}}\right]^T$. The entire process is then repeated until convergence. Note that the first part of Algorithm 1 is a heuristic scheme applied to identify a feasible solution, and no convergence guarantees can be provided. The second part of the algorithm converges monotonically (this is not necessarily the case for the first part), since it is a bilinear descent iteration; however, the limit point is not guaranteed to be the global optimum of the original bilinear problem.

Fig. 2 shows how the power dispatch of each unit and the obtained objective value change per iteration for the benchmark problem introduced in the next section. After three iterations the first part converges, whereas for the second only one iteration

is needed. As expected, the cost decreases monotonically in the second part.

B. Method 2: Convex Reformulation

Assume that, in the case where $i \in \mathcal{I}_G$, we can distinguish between the mismatch that corresponds to wind deviation and the one that occurs due to a generator outage by introducing different distribution vectors. For $i \in \mathcal{I}$, the power correction term would now be

$$R_t^i = d_{\mathrm{up},t}^{1,i} \max_{+}(P_{w,t}^f - P_{w,t}) - d_{\mathrm{down},t}^{1,i} \max_{+}(P_{w,t} - P_{w,t}^f) + d_{\mathrm{up},t}^{2,i} P_{G,t}^i.$$

By considering the optimization problem that corresponds to (1)–(8) if the additional distribution vectors are introduced, $d_{\mathrm{up},t}^{2,i} P_{G,t}^i$ becomes the only bilinear term, which appears both in the constraints and the objective function. Setting $z_t^i = d_{\mathrm{up},t}^{2,i} P_{G,t}^i \in \mathbb{R}^{N_G}$ and defining the new decision vector

$$\tilde{x}_t = [P_{G,t}, [d_{\mathrm{up},t}^i, d_{\mathrm{down},t}^i]_{i\in\mathcal{I}\setminus\mathcal{I}_G}, [d_{\mathrm{up},t}^{1,i}, d_{\mathrm{down},t}^{1,i}, z_t^i]_{i\in\mathcal{I}_G}, [R_{\mathrm{up},t}^i, R_{\mathrm{down},t}^i]_{i\in\mathcal{I}}]^T \in \mathbb{R}^{N_G+N_G^2+4N_G(N_{\mathrm{out}}+1)}$$

the resulting problem is linear in z_t^i and hence convex. It is of the same structure as (1)–(8) with the additional constraint

$$\mathbf{1}^T z_t^i = P_{G,t}^i, \qquad \text{for all } i \in \mathcal{I}_G. \tag{9}$$

Once the solution to this problem is computed, for all $i \in \mathcal{I}_G$, $d_{\mathrm{up},t}^{2,i}$ is calculated as $d_{\mathrm{up},t}^{2,i} = z_t^i / P_{G,t}^i$ if $P_{G,t}^i$ is not equal to zero and is set to zero otherwise. Note that the sum of the elements of $d_{\mathrm{up},t}^{2,i}$ is constrained to be one, since z_t^i, $i \in \mathcal{I}_G$ satisfies (9). For real time operation, the look-up table interpretation (discussed in Section II-C) may be used. Then, given a mismatch $P_{m,t}^i = (P_{w,t} - P_{w,t}^f) - P_{G,t}^i$, the participation of each unit in compensating $P_{m,t}^i$ can be computed as $R_t^i / \mathbf{1}^T R_t^i$. Note that, following this procedure, we convexify the bilinear terms inside the probability. The overall problem is still nonconvex, however, due to the presence of the chance constraint. In Section III-C, we elaborate on how to deal with this issue.

C. Solving the Chance Constrained Problem

1) The Scenario Approach: Applying method 2 directly transforms (1)–(8) to a problem where the constraints inside the chance constraints are convex. This is also the case at every iteration of method 1, with the difference that the size of the resulting problem might be different from that of method 2. In this section we provide a scenario based methodology to deal with the chance constraint while ensuring tractability of the resulting program. Since the decision variables of the different optimization stages are not coupled via the constraints or the objective function, we can treat each hour separately. The chance constrained problem that we need to solve can be then written in a more compact notation as

$$\begin{aligned} \min_{x\in\mathbb{R}^{N_x}} \quad & J(x) \\ \text{s.t.}: \quad & \mathbb{P}\Big(\delta \in \Delta \mid A(\delta)x + c(\delta) \le 0\Big) \ge 1-\epsilon, \end{aligned} \tag{$\mathcal{P}_1$}$$

where $x \in \mathbb{R}^{N_x}$ is the vector of decision variables with N_x being the dimension of x_t, $\delta \in \Delta \subset \mathbb{R}$ is the uncertain parameter (in this case the wind power $P_{w,t}$), $J(x) \in \mathbb{R}$ is quadratic in x, and A, c are of appropriate dimension. Using the standard scenario approach of [27] requires replacing the chance constraint with a finite number of hard constraints, each of them corresponding to a different uncertainty realization. This results in the following optimization problem:

$$\begin{aligned} \min_{x\in\mathbb{R}^{N_x}} \quad & J(x) \\ \text{s.t.}: \quad & A(\delta^{(k)})x + c(\delta^{(k)}) \le 0 \text{ for } k = 1,\dots,N, \end{aligned} \tag{$\mathcal{P}_1'$}$$

where $\delta^{(k)}$, $k = 1,\dots,N$ denote the different realizations of the uncertain parameter δ, extracted according to $\mathbb{P}$. The authors of [28] provide a bound on number N, of uncertainty realizations that one needs to generate to achieve probabilistic constraint violation guarantees. It is shown that, if we generate

$$N \ge \frac{2}{\epsilon}\Big(\ln\frac{1}{\beta} + N_x\Big) \tag{10}$$

realizations of the uncertainty, the resulting solution of $(\mathcal{P}_1')$ will satisfy the chance constraint in $(\mathcal{P}_1)$ with probability at least $1-\beta$; here, N_x is the number of decision variables and $\beta \in (0,1)$ is a confidence parameter. There are two basic limitations of this procedure. The number of scenarios (and hence also the number of constraints in $(\mathcal{P}_1')$) grows with respect to the number of decision variables and convexity of the objective function and the constraints of the initial problem is required. The latter prevents us from providing probabilistic performance guarantees to mixed-integer programs like those arising in unit commitment problems.

To overcome this difficulty, we exploit the recent results of [25]. Instead of directly using the scenario approach and solving $(\mathcal{P}_1')$, we construct and solve a robust version of $(\mathcal{P}_1)$ with interval bounded uncertainty, where the uncertainty bounds are computed at an intermediate step using the scenario approach. Specifically, we seek bounds $\tau = (\underline{\tau}, \overline{\tau}) \in \mathbb{R}^2$, such that $\delta \in [\underline{\tau}, \overline{\tau}]$ with probability at least $1-\epsilon$. Therefore, consider the optimization problem

$$\begin{aligned} \min_{\tau\in\mathbb{R}^2} \quad & (\overline{\tau} - \underline{\tau}) \\ \text{s.t.}: \quad & \mathbb{P}\Big(\delta \in \Delta \mid \delta \in [\underline{\tau}, \overline{\tau}]\Big) \ge 1-\epsilon. \end{aligned} \tag{$\mathcal{P}_2$}$$

This is a different chance-constrained problem, whose objective function and constraints are convex by construction. Therefore, we can determine its solution using the scenario approach. This requires solving the following problem:

$$\begin{aligned} \min_{\tau\in\mathbb{R}^2} \quad & (\overline{\tau} - \underline{\tau}) \\ \text{s.t.}: \quad & \delta^{(k)} \in [\underline{\tau}, \overline{\tau}], \qquad \text{for } k = 1,\dots,\widetilde{N}, \end{aligned} \tag{$\mathcal{P}_2'$}$$

where $\widetilde{N} \ge (2/\epsilon)\big(\ln(1/\beta) + 2\big)$ since $(\mathcal{P}_2)$ has only two decision variables. Note that $(\mathcal{P}_2')$ is effectively a selection problem

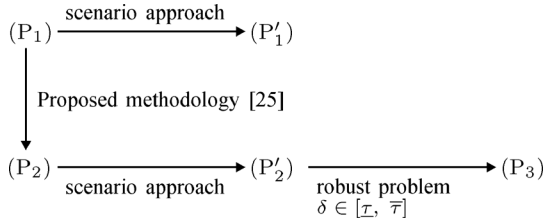

Fig. 3. Connection between problems $(\mathcal{P}_1) - (\mathcal{P}_3)$.

and $\overline{\tau}$, $\underline{\tau}$ correspond to the maximum and minimum, respectively, among the $\widetilde{N}$ generated samples. We then use the computed bounds to formulate the robust counterpart of $(\mathcal{P}_1)$ as

$$\begin{aligned} \min_{x\in\mathbb{R}^{N_x}} \quad & J(x) \\ \text{s.t.}: \quad & \max_{\delta\in[\underline{\tau},\,\overline{\tau}]} A(\delta)x + c(\delta) \leq 0. \end{aligned} \qquad (\mathcal{P}_3)$$

The maximization in $(\mathcal{P}_3)$ is interpreted element-wise. Note that $(\mathcal{P}_3)$ is no longer a stochastic program, but we require that its constraints be satisfied for all values of the uncertainty inside $[\underline{\tau},\ \overline{\tau}]$, where $\underline{\tau}$, $\overline{\tau}$ are computed by $(\mathcal{P}'_2)$. Therefore, $(\mathcal{P}_3)$ is a robust optimization problem (equivalently it could be thought of as a min-max problem) and can be solved efficiently using the algorithms of [29]. In particular, for the specific setup where the uncertainty is scalar, it suffices to enforce the constraints in (8) only for the extreme values $\underline{\tau}$, $\overline{\tau}$ of the uncertainty intervals, which correspond to the maximum and minimum, in a probabilistic sense, value of the wind power (see also [26]). Following [25], with confidence at least $1-\beta$, any feasible solution of $(\mathcal{P}_3)$ satisfies the chance constraint of $(\mathcal{P}_1)$. Since the chance constraint corresponding to each hour $t = 1, \ldots, T$ is satisfied with confidence at least $1-\beta$, all chance constraints would be simultaneously satisfied with confidence at least $1 - T\beta$ (see also [30]). The connection between the problems $(\mathcal{P}_1) - (\mathcal{P}_3)$ is shown in Fig. 3.

In contrast to the standard scenario approach, our methodology provides finite sample size guarantees regarding the probability of constraint satisfaction, convexity of the initial problem with respect to the decision variables. This implies that our method is applicable to all problems where $(\mathcal{P}_3)$ can be solved effectively. This includes convex problems, but also problems such as classes of mixed integer programs, for which effective robust optimization algorithms already exist [29]. This feature is exploited in [26], where the unit commitment problem is incorporated in the proposed framework.[2]

Including additional uncertainty sources (e.g., more wind power generators, load uncertainty) or introducing coupling constraints among the stages of the optimization problem (ramping constraints, minimum up-down times, etc.) would result in a problem where the uncertainty is no longer scalar. The preceding formulation would remain unaffected with the exception that the number of scenarios $\widetilde{N}$ would depend on the dimension of the uncertainty vector and that problem $(\mathcal{P}_3)$ would have hyper-rectangular instead of interval bounded uncertainty. Using the methodology of [29], the resulting optimization still leads to a tractable reformulation.

2) Quantile-Based Approach: An alternative way to treat the chance constraint is to consider the stationary distribution of the wind power error, as this is computed in Section IV-A. Two extreme scenarios are then considered: a low one corresponding to the forecast plus the $\epsilon/2$ percentile of the error distribution and a high one corresponding to the forecast plus the $(1 - \epsilon/2)$ percentile of the error distribution (that way we have the same ϵ-guarantees with the scenario approach). Now, treating the wind power as a bounded uncertainty, with the bounds corresponding to these two extreme cases, we compute the generation dispatch and the reserves by solving the robust counterpart of (1)–(8), where the bilinear constraints are tackled using either method 1 or method 2. As in the previous approach, due to the particular structure of the problem, it suffices to enforce the constraints in (8) only for the two extreme values of the wind power, computed as described above. Note that the resulting problem is of the same type as the one that we need to solve when using the scenario approach of the previous section, with the difference that the extreme values of the wind power are not necessarily the same for both methods.

D. Probabilistic Performance Guarantees

Based on the method we use to deal with the bilinearity problem and the approach we adopt to tackle the chance constraint, we can offer different probabilistic performance guarantees. If method 1 is selected to deal with the bilinear constraints, we need to employ the scenario or the quantile-based approach at every iteration of the heuristic algorithm. The resulting solution (if convergence at the first part of Algorithm 1 occurs) will be feasible by construction for the bilinear problem. Therefore, applying either the scenario or the quantile-based approach, we have probabilistic guarantees that the resulting optimal solution is feasible for the initial chance constrained problem (1)–(8).

Consider now the case where method 2 is used to transform the bilinear constraints to convex ones. Following the scenario approach results in solving the robust problem $(\mathcal{P}_3)$, whose solution is feasible for $(\mathcal{P}_1)$ with confidence at least $1-\beta$. However, we have no guarantees that the resulting solution is feasible for the bilinear chance constrained problem (1)–(8). In the particular case where the uncertainty at every stage of the optimization problem is scalar, it is shown in Appendix A that, using method 2, we obtain probabilistic guarantees regarding the satisfaction of the constraints of (1)–(8).

IV. Simulation Study

A. Wind Power Model and Simulation Setup

We assume that the wind power is the sum of a deterministic component (forecast) and a stochastic one, which models the error between the forecast and the actual wind power. To generate scenarios for the wind power error, we employed the

[2]Including the unit commitment problem in the proposed probabilistic framework would require the introduction of a vector $u \in \{0,1\}^{N_G}$ of binary variables to encode the "ON–OFF" status of the generating units. This would give rise to a term Bu additive to the left-hand side of the inequality inside the chance constraint of problems $(\mathcal{P}_1)$, $(\mathcal{P}'_1)$, and $(\mathcal{P}_3)$, where $B \in \mathbb{R}^{N_x \times N_G}$ would be a matrix with constant entries. The resulting problem $(\mathcal{P}_3)$ would be a robust mixed-integer quadratic program since it would involve optimizing over both x and u and can be tackled using the algorithms of [29].

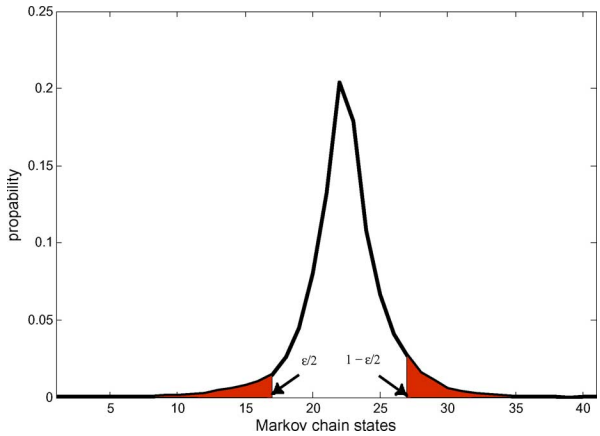

Fig. 4. Stationary distribution of the wind power error. The "shaded" regions denote the quantiles, which contain an ϵ fraction of the probability mass, whereas the arrows indicate the $\epsilon/2$ and $(1-\epsilon/2)$ percentiles.

approach of [31], which proposes a Markov chain model to generate wind power time series that take into account the temporal correlation of the wind power error. We used five-year, hourly measured data (both actual and forecasted values), for the aggregated wind power production of Germany over the period 2006–2011. Discretizing the wind power error with 41 states, we construct the transition probability matrix $\bar{P}$ for the wind power error. It exhibits a pronounced block-triangular structure suggesting strong auto-correlation of the wind power error. The stationary distribution π of the wind power error is computed as a vector whose entries are all non-negative, sum up to one, and satisfy $\pi = \bar{P}^T\pi$. Fig. 4 shows the stationary distribution π of the wind power error, where the shaded regions denote the quantiles which contain an ϵ fraction of the probability mass.

To evaluate the performance of our approach we applied it to the IEEE 30-bus network [22], which includes $N_b = 30$ buses, $N_G = 6$ generators, $N_l = 41$ lines, and is modified to include a wind power generator connected to bus 22. All numerical values for the network data are retrieved from [22]. Even though it is not a large scale system, using the IEEE 30-bus network enables us to illustrate some features of the proposed methodology. However, the proposed approach can be applied to larger scale systems at manageable computational costs.

For all simulations we used $\epsilon = 10^{-1}$ and $\beta = 10^{-4}$. Note that when using the scenario approach, decreasing the value of ϵ leads to a higher number of scenarios. However, using the procedure described in Section III-C.1 we only need the scenarios to solve Problem $(\mathcal{P}_2')$, which is effectively a selection problem and thus easy to solve. The size of problem $(\mathcal{P}_3)$ is of importance and this is independent from the number of scenarios. The number of scenarios will just determine (in a probabilistic sense) the size of the interval uncertainty bounds and hence the conservatism of the resulting solution (the lower the value of ϵ the more conservative the solution of $(\mathcal{P}_3)$ tends to be). Therefore, our choice for ϵ serves as a compromise between the theoretical guarantees we can offer and the conservatism of the resulting solution, as this is quantified by an a posteriori analysis and is not related to the computational cost of solving $(\mathcal{P}_3)$.

To collect statistical results regarding the performance of our algorithm, we carried out a Monte Carlo study, evaluating the solution of (1)–(8) (reformulated based on the proposed alternatives, i.e., method 1 and 2, scenario and quantile approach) against 10,000 wind power realizations, not included in the optimization process. Using the obtained reserve strategy (i.e., the power correction term (2) with the distribution vectors fixed according to the outcome of the optimization problem and the wind power equal to the evaluation scenario), for each of these realizations we examined whether the problem constraints are satisfied. Note that since we examine the feasibility of all constraints, all possible outages are taken into account in the evaluation phase. Since we perform a probabilistic design, applying our reserve strategy still allows for constraint violation but with a certain probability. By constraint violation we mean the case where the wind power realization used to evaluate our solution leads to a power mismatch for which at least one of the constraints is violated. Such a violation does not necessarily correspond to the base case but to some $i = 0, \ldots, N_{out}$. In case we violate the constraints and end up with an excess of power, we refer to the maximal such amount as power surplus, which corresponds to a potential wind power curtailment action. In the opposite case we use the term power deficit to characterize the amount of power that may not be covered by the scheduled up-spinning reserves. In the realistic setup of an interconnected system a fraction of this amount would be provided by the primary frequency reserves of neighboring areas (assuming the primary reserves of our area are also at saturation). If these primary reserves are not sufficient to cover the power deficit load shedding will occur. Following its definition, if no power deficit is encountered the system will always be N − 1 secure.

Note that for the simulation study of the next section we differentiate among the distribution vectors based on the sign of the wind power error and the possible generator outage, thus having the same vector for all line and load outages. Our choice is motivated by a desire to minimize the number of decision variables (and hence the computational cost) in the optimization problem.

All optimization problems were solved using the solver CPLEX [32] via the MATLAB interface YALMIP [33].

B. Simulation Results

We first investigate the performance of methods 1 and 2 when applying both the scenario approach and the quantile based approach for one day of our data. Fig. 5(a) shows the forecast ("blue") and the actual ("red") wind power, the wind power scenarios ("green") that were used for the scenario approach (generated according to $\widetilde{N}$), and the wind power quantiles that were used for the quantile based approach. For the analysis of Fig. 5(c) the solution of (1)–(8) was evaluated using the actual wind power realization (red curve in Fig. 5(a)). Figs. 6, 7 provide statistical information regarding the performance of our methods using 10,000 wind power realizations, that were used for evaluation purposes and their span corresponds to the shaded region of Fig. 5(a).

Fig. 5(b) shows the scheduled cost (production + reserves) for the convex reformulation ("dashed" line) and the heuristic algorithm ("solid" line), using both the scenario and the quantile based approach. All methods lead to a similar cost, but the quantile based ones result in slightly lower values. The difference in the cost occurs due to the fact that the quantile based

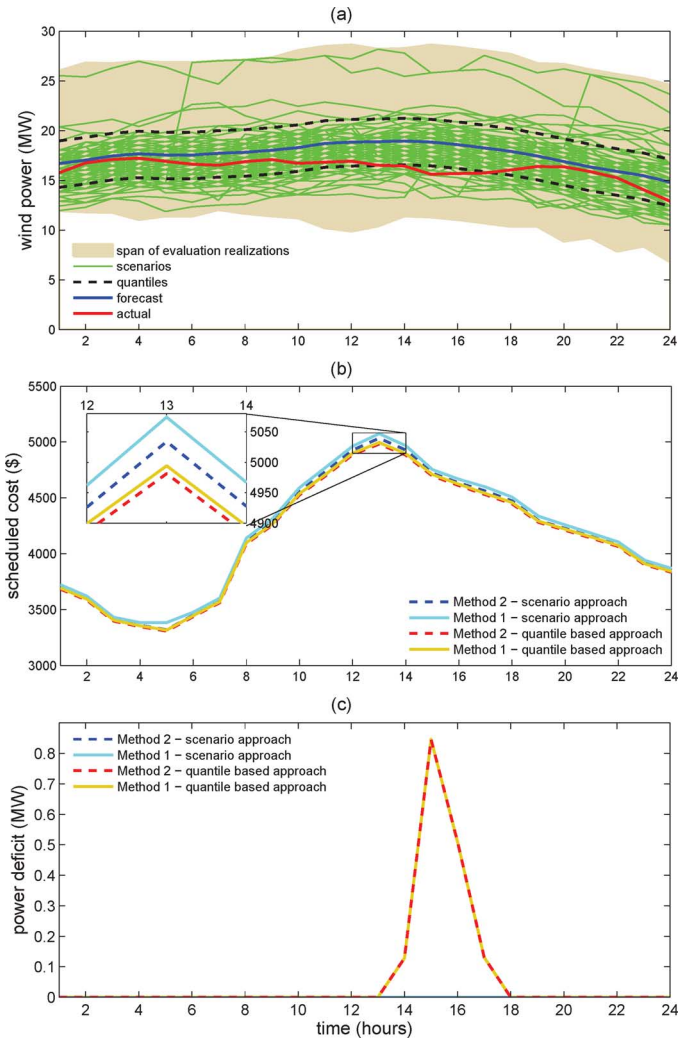

Fig. 5. (a) Wind power for one day of the simulated data. Forecast ("blue"), actual ("red"), scenarios used for methods 1 and 2 ("green"), and the span of the 10,000 wind power realizations used for evaluation purposes (shaded region). (b) Total scheduled cost (production + reserves) for method 1 ("solid" line) and method 2 ("dashed" line). The "blue" and "light blue" curves correspond to the scenario approach, whereas the "red" and "yellow" to the quantile based approach. (c) Power deficit for method 1 ("solid" line) and method 2 ("dashed" line). The "blue" and "light blue" curves correspond to the scenario approach, whereas the "red" and "yellow" to the quantile based approach.

approach leads to scheduling less reserves, since it does not capture extreme scenarios like the scenario approach. However, this is at the expense of more frequent constraint violations (see also Figs. 6, 7). The latter is highlighted in Fig. 5(c) which shows the amount of power deficit for each method, as this occurs once the actual wind is realized. Using the scenario approach neither method 1 nor method 2 lead to a power deficit, whereas the for the quantile based approach the amount of deficit is the same for both methods. As discussed below, this is not the case in general. No power surplus was encountered since the actual wind scenario never exceeds the upper quantile barrier.

For comparison purposes we solved the nonlinear problem (1)–(8) directly using the nonlinear solver IPOPT. In all cases the resulting solution led in slightly lower cost values compared to method 1, with a maximum difference of 1%. Therefore, method 1 provides a reliable alternative to more direct schemes based on nonlinear solvers, since it leads to a similar cost while involving the solution of a sequence of convex problems. method 2 leads to slightly lower cost compared to the nonlinear solver (maximum difference of at most 1%). This is due to the fact that our setup satisfies the requirements of Proposition 1 in Appendix A; hence, method 2 provides an exact convex reformulation of the bilinear problem. This implies that these problems have the same optimal objective values, however, we do not have guarantees that the bilinear one (solved using the nonlinear solver) can be solved up to optimality. In the general case, where the requirements of Proposition 1 are not satisfied, method 2 will not necessarily outperform the solution of the nonlinear solver in terms of cost since it will only be a convex relaxation of the bilinear problem. However, since method 2 leads to a convex problem the computational cost will be much lower.

Methods 1 and 2 lead to different distribution of the reserves among the various generators and to different total amount of reserves in general. Therefore, the amount of power deficit or surplus differs according to whether method 1 or 2 is employed. Figs. 6(a) and (c) and 7(a) and (c) show the power surplus and power deficit for the scenario approach and the quantile-based approach, respectively, when method 2 is used.[3] The results for method 1 are similar and are omitted in the interest of space. However, the probability of constraint violation (power deficit or surplus) depends solely on the wind power used for evaluation purposes. To see this, notice that the left or right hand-side inequalities of the last constraint inside (8) will always hold with equality for at least one of its rows (possibly different rows for methods 1 and 2). From the definition of the power correction term, this implies that any wind power realization outside the span of the scenarios used for the scenario approach or the "band" of the quantile-based approach will result in violating these specific constraints. Therefore, the distributions shown in Figs. 6(b) and (d) and 7(b) and (d) are the same both for methods 1 and 2. The probabilities of these figures are calculated as the fraction of the 10 000 evaluation scenarios that resulted in power surplus and deficit, respectively. The empirical probability of constraint violation is determined by the sum of the individual probabilities of power surplus and deficit. The quantile-based approach, even though it provides the same ϵ-type theoretical guarantees, leads to systematically more power deficit and surplus since the scenarios ("green") span the entire range of the shaded region, which includes the wind power realizations that were used for evaluation purposes. It should be noted that load shedding and wind power curtailment becomes more prominent at later times due to accumulated forecast inaccuracy. This is more pronounced when using the quantile-based approach (Fig. 7) since the robustness guarantees offered by this approach are limited in a band ["dashed" black lines in Fig. 5(a)] which has the same width irrespective of the time instance (it is based only on the stationary distribution of the wind power error). Therefore, since the wind power inaccuracy is increasing with time while the robustness region remains constant, we have the increasing pattern of Fig. 7. On the other hand, since the scenario

[3]In the boxplots, the "red" line corresponds to the median value, the edges of the box correspond to the 25th and 75th percentiles, whereas the whiskers extend to a 99% coverage. The "red" marks denote the data outliers, which lie outside the 99% confidence region.

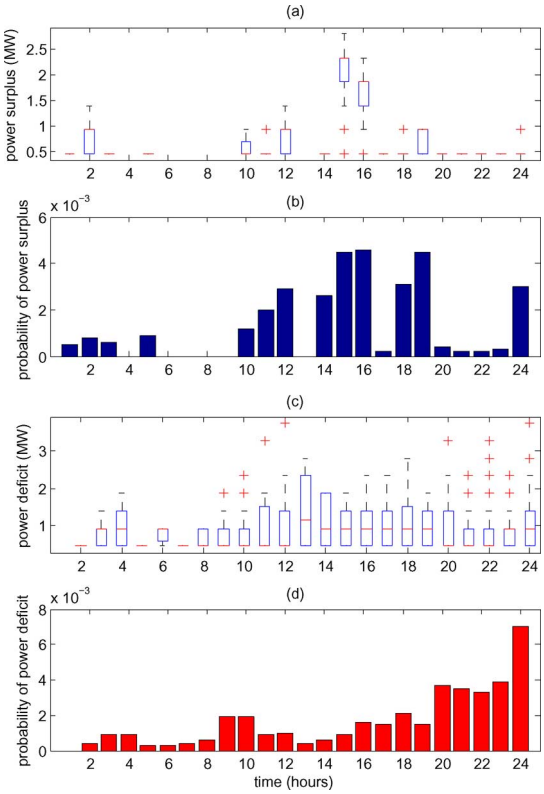

Fig. 6. Power deficit and surplus using the scenario approach, for one day of the simulated data, evaluated with 10,000 wind power realizations ($\epsilon = 10^{-1}$ and $\beta = 10^{-4}$). (a) Power surplus for method 2. (b) Probability of power surplus. (c) Power deficit for method 2. (d) Probability of power deficit.

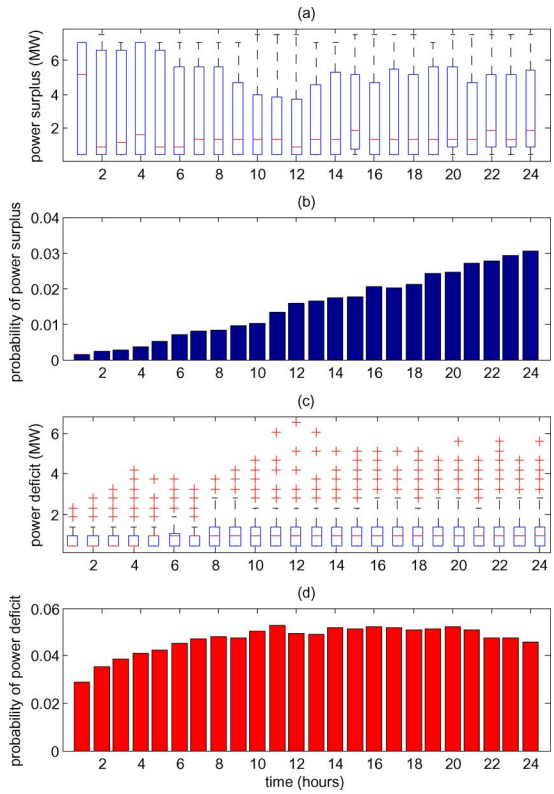

Fig. 7. Power deficit and surplus using the quantile based approach, for one day of the simulated data, evaluated with 10,000 wind power realizations ($\epsilon = 10^{-1}$ and $\beta = 10^{-4}$). (a) Power surplus for method 2. (b) Probability of wind power surplus. (c) Power deficit for method 2. (d) Probability of power deficit.

approach (Fig. 6) is based on sampling, the span of the scenarios ["green" trajectories in Fig. 5(a)] does not exhibit this regularity pattern and covers a wider range of wind power values.

Using the scenario approach, Fig. 8 depicts the distribution of the percentage of cost improvement, using method 1 against method 2 for 30 days of hourly measured data. Method 2 systematically leads to lower cost compared with method 1 since, as discussed above, it falls in the framework of Appendix A. However, we cannot generalize this pattern if the setup of Appendix A is not satisfied. The total amount of power deficit (surplus) for the 30 days, evaluated with the actual wind power realizations, was 37 (3) MW for method 1 and 43 (3) MW for method 2.

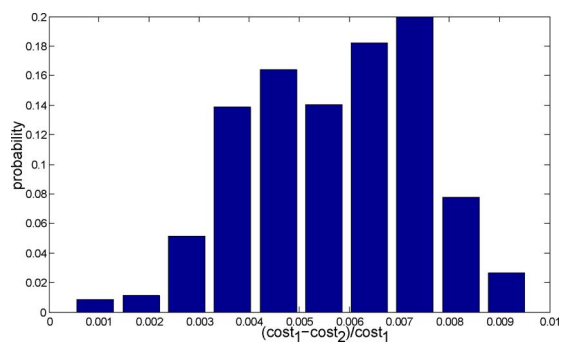

Fig. 8. Distribution of the percentage of cost improvement, using the scenario approach, and applying method 1 against method 2 for 30 days of hourly measured data.

C. Simulation Conclusions

The main conclusions drawn from our simulation results are summarized in Table I. As already mentioned, the probability of power deficit or surplus depends only on the approach used to solve the chance-constrained problem and not on methods 1 or 2, thus justifying the same characterization in the corresponding entries of Table I. The same holds for the conservatism of each method. By inspection of Figs. 6 and 7 it can be observed that the probability of power deficit or surplus when the scenario approach is used is lower compared to the one obtained by the quantile based approach, while both methods are below the design value of ϵ. This implies that the scenario approach leads to a more conservative performance compared to the quantile based approach. This is justified by the fact that the scenario approach is based on sampling, so outliers may appear in the optimizations process, and by the fact that the bound which determines the number of scenarios $\widetilde{N}$ is not tight. To rank the methods in terms of cost we use a numbering scheme where "1" implies low and "4" high cost. Independently of the approach used to solve the chance constraint, method 2 leads to lower cost compared to method 1 since it constitutes a convex reformulation of the initial problem (see also Appendix A). Using the quantile based approach results in scheduling less reserves, thus leading to a lower scheduled cost.

Even though it seems more conservative in some cases, the scenario approach provides a more general framework to handle uncertainty since it takes into account the temporal correlation

TABLE I
COMPARISON OF THE PROPOSED ALTERNATIVE APPROACHES IN TERMS OF COST, POWER DEFICIT, POWER SURPLUS AND THE DEGREE OF CONSERVATISM.

Approach	power surplus	power deficit
Meth. 1 + scenarios	lower	lower
Meth. 2 + scenarios	lower	lower
Meth. 1 + quantiles	higher	higher
Meth. 2 + quantiles	higher	higher

Approach	conservatism	scheduled cost
Meth. 1 + scenarios	higher	4
Meth. 2 + scenarios	higher	3
Meth. 1 + quantiles	lower	2
Meth. 2 + quantiles	lower	1

of the wind power error. This is of major importance especially if the optimization stages are coupled, as in the case where ramping constraints of the generating units are taken into account. Moreover, subsequent developments of the scenario approach [34], which are not exploited in this paper, provide a way to reduce the conservatism while providing the same performance guarantees.

V. CONCLUDING REMARKS

In this paper, a new methodology for solving security-constrained reserve scheduling problems for systems with fluctuating generation is presented. Moreover, a corrective security control scheme consisting of a reserve strategy that could be applied in real-time operation is introduced, and different alternatives to deal with the resulting chance-constrained bilinear problem are proposed.

Despite the fact that we focus on secondary frequency control reserves, the proposed methodology could also be applied to determine the primary and tertiary reserves. Such an implementation is currently under investigation. Moreover, we focus on decentralizing the developed algorithm and on exploiting the work of [35], [36], by including a convex ac optimal power flow relaxation. Another issue is to investigate the validity of our approach for alternative market structures [37] and compare it with other benchmark methods.

APPENDIX
DISCUSSION ON METHOD 2

Here, we focus on a specific setup where the uncertainty at every stage of the optimization problem is scalar. We will show how method 2 can be used in conjunction with the scenario approach (similar arguments hold for the quantile-based approach as well) to provide feasibility guarantees for problem (1)–(8). Since the scenario-based methodology of Section III-C does not require convexity of the underlying problem, with confidence of at least $1-\beta$, the optimal solution of the robust counterpart of (1)–(8) is feasible for the initial chance-constrained problem. Note that, for each optimization stage, the robust version of (1)–(8) has interval bounded uncertainty and bilinear constraints and denote by J^* the optimal cost corresponding to this problem. We will show how to construct the optimal solution of this problem so as to obtain the desired probabilistic guarantees.

Using method 2, the robust counterpart of (1)–(8) can be transformed to a robust problem with linear constraints. Denote $\widetilde{J}^*$ as the optimal cost of the resulting robust problem. Proposition 1 below shows that for this particular setup the costs J^* and $\widetilde{J}^*$ are equal, and an optimal solution that corresponds to $\widetilde{J}^*$ can be used to construct an optimal solution corresponding to J^*. This implies that it suffices to compute a solution that leads to $\widetilde{J}^*$ (this is a robust convex problem and can be solved using the approach of [29]) and use it to determine an optimal solution of the robust version of (1)–(8), thus inheriting the probabilistic guarantees of the scenario approach.

Proposition 1: If the uncertainty at every stage of (1)–(8) is scalar, then $J^* = \widetilde{J}^*$. Moreover, a solution that corresponds to $\widetilde{J}^*$ can be used to construct a solution that corresponds to J^*.

Proof:

Part 1: $J^* \geq \widetilde{J}^*$: For every outage $i \in \mathcal{I}_G$, method 2 introduces different distribution vectors $d^{1,i}_{\mathrm{up},t}$, $d^{2,i}_{\mathrm{up},t}$ to distinguish between the mismatch which occurs due to wind deviation and the one due to a generator outage. Therefore, the setup of problem (1)–(8) is a special case of method 2, corresponding to the situation where for $i \in \mathcal{I}_G$, $d^{1,i}_{\mathrm{up},t} = d^{2,i}_{\mathrm{up},t}$. The latter implies that by construction the cost of the solution obtained by method 2 is never higher compared to the one of (1)–(8) since we have more degrees of freedom.

Part 2: $J^* \leq \widetilde{J}^*$: Since the stages are decoupled we can focus on specific time instance t. Consider the terms $P_{G,t}$, $[d^i_{\mathrm{up},t}, d^i_{\mathrm{down},t}]_{i\in\mathcal{I}\setminus\mathcal{I}_G}$, $[R^i_{\mathrm{up},t}]_{i\in\mathcal{I}}$, $[R^i_{\mathrm{down},t}]_{i=0}^{N_{out}}$ of the optimal solution of method 2. It suffices to show that for all $i \in \mathcal{I}_G$ there exist vectors $d^i_{\mathrm{up}}, d^i_{\mathrm{down}} \in \mathbb{R}^{N_G}$, which together with these terms, constitute a feasible solution of the robust counterpart of (1)–(8). This solution would satisfy all of the constraints in (8) for all values of the uncertainty inside the interval (scalar uncertainty was assumed) where it is confined. Due to linearity of the constraints with respect to the uncertainty, it suffices to check feasibility only for the extreme values of this interval, which is denoted here by $[\underline{P}_{w,t},\ \overline{P}_{w,t}]$. We show this here only for the case where $\underline{P}_{w,t} \leq P^f_{w,t}$ that results in determining $[d^i_{\mathrm{up}}]_{i\in\mathcal{I}_G}$, whereas the proof for the other case is similar. Moreover, the cost of the constructed solution will be equal to $\widetilde{J}^*$ since the cost depends only on $P_{G,t}$ and $[R^i_{\mathrm{up},t}, R^i_{\mathrm{down},t}]_{i\in\mathcal{I}}$. The claim follows then directly, since we will have identified a feasible but not necessarily optimal solution for (1)–(8).

To construct such a feasible solution, notice that, in all constraints, the distribution vectors appear through the term R^i_t. Therefore, consider $[d^i_{\mathrm{up}}]_{i\in\mathcal{I}_G}$ such that the power correction term of the bilinear problem (see (2) for $\underline{P}_{w,t} \leq P^f_{w,t}$) is equal to the one obtained by method 2, i.e., for all $i \in \mathcal{I}_G$

$$d^i_{\mathrm{up}}(P^f_{w,t} - \underline{P}_{w,t} + P^i_{G,t}) = d^{1,i}_{\mathrm{up},t}(\underline{P}^f_{w,t} - P_{w,t}) + d^{2,i}_{\mathrm{up},t}P^i_{G,t}. \quad (11)$$

If, in addition, $\mathbf{1}^T d^i_{\mathrm{up}} = 1$, then all other constraints of (1)–(8) will be trivially satisfied, since they are the same with those of method 2. By multiplying both sides of (11) with $\mathbf{1}^T$, we obtain

$$\mathbf{1}^T d^i_{\mathrm{up}}(P^f_{w,t} - \underline{P}_{w,t} + P^i_{G,t}) = \mathbf{1}^T d^{1,i}_{\mathrm{up},t}(P^f_{w,t} - \underline{P}_{w,t}) + \mathbf{1}^T d^{2,i}_{\mathrm{up},t}P^i_{G,t}.$$

Since $z_t^i = d_{\mathrm{up},t}^{2,i} P_{G,t}^i$, the last statement is equivalent to $\mathbf{1}^T d_{\mathrm{up}}^i (P_{w,t}^f - \underline{P}_{w,t} + P_{G,t}^i) = \mathbf{1}^T d_{\mathrm{up},t}^{1,i} (P_{w,t}^f - \underline{P}_{w,t}) + \mathbf{1}^T z_t^i$. However, we have that $\mathbf{1}^T d_{\mathrm{up}}^{1,i} = 1$ and $\mathbf{1}^T z_t^i = P_{G,t}^i$. Hence, $\mathbf{1}^T d_{\mathrm{up}}^i = 1$ concluding the proof. ∎

Note that the assumption of scalar uncertainty was used at the second part of the proof, since, by checking only the two extreme values of the interval bounded uncertainty, we were able to have a unique map from $d_{\mathrm{up},t}^{1,i}$, $d_{\mathrm{up},t}^{2,i}$ to d_{up}^i, d_{down}^i, $i \in \mathcal{I}_G$. In case the uncertainty is of higher dimension, this proof is not always valid, unless we introduce additional distribution vectors for every vertex of the uncertainty set.

ACKNOWLEDGMENT

The authors would like to thank Fraunhofer IWES in Kassel for providing the wind power data, Dr. J. Mathiew for proofreading the manuscript, and the anonymous reviewers for their detailed comments that significantly improved the context of the paper.

REFERENCES

[1] P. Kundur, J. Paserba, V. Ajjarapu, G. Andersson, A. Bose, C. Canizares, N. Hatziargyriou, D. Hill, A. Stankovic, C. Taylor, T. V. Cutsem, and V. Vittal, "Definition and classification of power system stability," *IEEE Trans. Power Syst.*, vol. 19, no. 3, pp. 1387–1401, Aug. 2004.

[2] K. Morison, P. Kundur, and L. Wang, "Critical issues for successful on-line security assessment," in *Real-Time Stability in Power Systems*, S. Savulescu, Ed. New York, NY, USA: Springer, 1986, pp. 147–166.

[3] B. Stott, O. Alsac, and A. Monticelli, "Security analysis and optimization," *Proc. IEEE*, vol. 75, no. 12, pp. 1623–1644, Dec. 1986.

[4] M. Zima, "Contributions to security of electric power systems," Ph.D. dissertation, Dept. Electr. Eng., ETH Zürich, Zürich, Switzlerland, 2006.

[5] G. Hug-Glanzmann, "Coordinated Power Flow Control to Enhance Steady-State Security in Power Systems," PhD, ETH Zürich, , 2008.

[6] G. Hug-Glanzmann and G. Andersson, "N − 1 security in optimal power flow control applied to limited areas," *IET Gen., Transm. Distrib.*, vol. 3, no. 2, pp. 206–215, 2009.

[7] F. Yang, A. Meliopoulos, G. Kokkinides, and G. Stefopoulos, "Security-constrained adequacy evaluation of bulk power system reliability," in *Proc. Int. Conf. Probabilistic Methods Appl. Power Symp.*, 2006, pp. 1–8.

[8] F. Milano, C. Canizares, and M. Invernizzi, "Voltage stability constrained OPF market models considering n − 1 contingency criteria," *Electric Power Syst. Res.*, vol. 74, no. 1, pp. 27–36, 2005.

[9] F. Bouffard and F. Galiana, "Stochastic security for operations planning with significant wind power generation," *IEEE Trans. Power Syst.*, vol. 23, no. 2, pp. 306–316, May 2008.

[10] S. Grijalva, S. Dahman, K. Patten, and A. Visnesky, Jr, "Large-scale integration of wind generation including network temporal security analysis," *IEEE Trans. Energy Convers.*, vol. 22, no. 1, pp. 181–188, Jan. 2007.

[11] A. Ahola, L. Haarla, J. Matilainen, and B. Lemström, "Wind power and the (N − 1) security of the Finnish transmission grid – A simulation study," in *Proc. Eur. Wind Energy Conf. and Exhibition*, 2009, pp. 1–10.

[12] G. Papaefthymiou, J. Verboomen, P. Schavemaker, and L. van der Slouis, "Impact of stochastic generation in power systems contingency analysis," in *Proc. Int. Conf. Probabilistic Methods Appl. to Power Symp.*, 2006, pp. 1–6.

[13] F. D. Galiana, F. Bouffard, J. M. Arroyo, and J. F. Restrepo, "Scheduling and pricing of coupled energy and primary, secondary, and tertiary reserves," *Proc. IEEE*, vol. 93, no. 11, pp. 1970–1983, Nov. 2005.

[14] F. Bouffard, F. Galiana, and A. Conejo, "Market-clearing with stochastic security- Part I: Formulation," *IEEE Trans. Power Syst.*, vol. 20, no. 4, pp. 1818–1826, Nov. 2005.

[15] F. Bouffard, F. Galiana, and A. Conejo, "Market-clearing with stochastic security- Part II: Case studies," *IEEE Trans. Power Syst.*, vol. 20, no. 4, pp. 1818–1826, Nov. 2005.

[16] F. Bouffard and F. Galiana, "Stochastic security for operations planning with significant wind power generation," *IEEE Trans. Power Syst.*, vol. 23, no. 2, pp. 306–316, May 2008.

[17] J. M. Morales, A. Conejo, and J. Pérez-Ruiz, "Economic valuation of reserves in power systems with high penetration of wind power," *IEEE Trans. Power Syst.*, vol. 24, no. 2, pp. 900–910, May 2009.

[18] A. Papavasiliou, S. Oren, and R. O'Neill, "Reserve requirements for wind power integration: A scenario-based stochastic programming framework," *IEEE Trans. Power Syst.*, vol. 26, no. 4, pp. 2197–2206, Nov. 2011.

[19] M. Vrakopoulou, K. Margellos, J. Lygeros, and G. Andersson, "Probabilistic guarantees for the N − 1 security of systems with wind power generation," in *Proc. Int. Conf. Probabilistic Methods Appl. Power Symp.*, 2012, pp. 858–863.

[20] B. Stott and O. Alsac, "Optimal power flow—A brief anatomy," in *Proc. XII Symp. Specialists in Electric Operational and Expansion Planning*, 2012, pp. 1–13.

[21] K. Margellos, T. Haring, P. Hokayem, M. Schubiger, J. Lygeros, and G. Andersson, "A robust reserve scheduling technique for power systems with high wind penetration," in *Proc. Int. Conf. Probabilistic Methods Appl. to Power Symp.*, 2012, pp. 870–875.

[22] R. D. Zimmerman, C. E. Murillo-Sanchez, and R. J. Thomas, "MATPOWER: Steady-state operations, planning, and analysis tools for power systems research and education," *IEEE Trans. Power Syst.*, vol. 26, no. 1, pp. 12–19, Feb. 2011.

[23] ENTSO-E, "Policy 3: Operational Security," 2009.

[24] G. Andersson, *Modeling and Analysis of Power Systems*. Zürich, Switzerland: ETH Zürich, 2011, Lecture Notes.

[25] K. Margellos, P. Goulart, and J. Lygeros, "On the road between robust optimization and the scenario approach for chance constrained optimization problems," *IEEE Trans. Automat. Control*, submitted for publication.

[26] K. Margellos, V. Rostampour, M. Vrakopoulou, M. Prandini, G. Andersson, and J. Lygeros, "Stochastic unit commitment and reserve scheduling: A tractable formulation with probabilistic certificates," in *Proc. Eur. Control Conf.*, 2013.

[27] G. Calafiore and M. C. Campi, "The scenario approach to robust control design," *IEEE Trans. Automat. Control*, vol. 51, no. 5, pp. 742–753, May 2006.

[28] M. C. Campi, S. Garatti, and M. Prandini, "The scenario approach for systems and control design," *Annu. Rev. Control*, vol. 33, no. 1, pp. 149–157, 2009.

[29] D. Bertsimas and M. Sim, "Tractable approximations to robust conic optimization problems," *Math. Programming, Series B*, vol. 107, pp. 5–36, 2006.

[30] K. Margellos, "Constrained optimal control for complex systems—Analysis and applications," Ph.D. dissertation, Dept. Electr. Eng., ETH Zürich, Zürich, Switzerland, 2012.

[31] G. Papaefthymiou and B. Klöckli, "MCMC for wind power simulation," *IEEE Trans. Energy Convers.*, vol. 23, no. 1, pp. 234–240, 2008.

[32] *"CPLEX11.0 Users Manual,"* ILOG.SA., Gentilly, France, 2008.

[33] J. Löfberg, "YALMIP: A toolbox for modeling and optimization in MATLAB," in *Proc. IEEE Int. Symp. Comput.-Aided Control Symp. Design*, 2005, pp. 284–289.

[34] M. Campi and S. Garatti, "A sampling-and-discarding approach to chance-constrained optimization: Feasibility and optimality," *J. Optim. Theory Applicat.*, vol. 148, no. 2, pp. 257–280, 2011.

[35] J. Lavaei and S. H. Low, "Zero duality gap in optimal power flow problem," *IEEE Trans. Power Syst.*, vol. 27, no. 1, pp. 92–107, Feb. 2012.

[36] B. Zhang and D. Tse, "Geometry of injection regions of power networks," 2012. [Online]. Available: http://arxiv.org/abs/1107.1467

[37] Y. Tan and D. Kirschen, "Co-optimization of energy and reserve in electricity markets with demand-side participation in reserve services," in *Proc. Power Symp. Conf. Expo.*, 2006, pp. 1182–1189.

Maria Vrakopoulou (S'09) received the Diploma in electrical and computer engineering from the University of Patras, Patras, Greece, in 2008. She is currently working toward the Ph.D. degree at the Power Systems Laboratory, Department of Electrical Engineering and Information Technology, ETH Zurich, Zurich, Switzerland.

Her research interests concentrate on the analysis, control and planning of power systems under uncertainty.

Kostas Margellos (S'09) received the Diploma in electrical and computer engineering from the University of Patras, Patras, Greece, in 2008, and the Ph.D. degree in automatic control from ETH Zurich, Zurich, Switzerland, in 2012.

Since December 2012, he is a Postdoctoral Researcher with the Automatic Control Laboratory, ETH Zurich, Zurich, Switzerland. His research interests include analysis and control of complex systems, with applications to stochastic scheduling problems for power networks with renewable generation.

John Lygeros (S'91–M'97–SM'06–F'11) received the B.Eng. degree in electrical engineering and M.Sc. degree in systems control from Imperial College of Science Technology and Medicine, London, U.K., in 1990 and 1991, respectively, and the Ph.D. degree from the University of California, Berkeley, CA, USA, in 1996.

He is a Professor of computation and control with the ETH Zurich, Zurich, Switzerland, and is currently serving as the Head of the Automatic Control Laboratory. During the period 1996–2000, he held a series of research appointments at the National Automated Highway Systems Consortium, Berkeley, CA, USA, the Laboratory for Computer Science, Massachusetts Institute of Technology, Cambridge, MA, USA, and the Department of Electrical Engineering and Computer Sciences, University of California. Between 2000 and 2003, he was a University Lecturer with the Department of Engineering, University of Cambridge, Cambridge, U.K., and a Fellow of Churchill College. Between 2003 and 2006, he was an Assistant Professor with the Department of Electrical and Computer Engineering, University of Patras, Patra, Greece. In July 2006, he joined the Automatic Control Laboratory at ETH Zurich, first as an Associate Professor, and since January 2010, he has been a Full Professor. His research interests include modeling, analysis, and control of hierarchical, hybrid, and stochastic systems, with applications to biochemical networks, automated highway systems, air traffic management, power grids, and camera networks.

Dr. Lygeros is a member of the Institution of Engineering and Technology, U.K., and the Technical Chamber of Greece.

Göran Andersson (M'86–SM'91–F'97) obtained his M.S. (1975) and Ph.D. (1980) degrees from the University of Lund, Sweden. In 1980 he joined ASEA's, now ABB's, HVDC division in Ludvika, Sweden, and in 1986 he was appointed full professor in electric power systems at KTH (Royal Institute of Technology), Stockholm, Sweden. Since 2000 he is full professor in electric power systems at ETH Zurich (Swiss Federal Institute of Technology), where he also heads the powers system laboratory. His research interests include power systems dynamics and control, power markets, and future energy systems.

Göran Andersson is fellow of the Royal Swedish Academy of Sciences, and of the Royal Swedish Academy of Engineering Sciences. He was the recipient of the IEEE PES Outstanding Power Educator Award 2007 and of the George Montefiore International Award 2010.